5-2022

Black Carbon Dominated Dust in Recent Radiative Forcing on Rocky Mountain Snowpacks

Kelly E. Gleason
Portland State University, k.gleason@pdx.edu

Joseph R. McConnell
Desert Research Institute

Monica M. Arienzo
Desert Research Institute

Graham Sexstone
USGS, Colorado Water Science Center

Stefan Rahimi
University of California Los Angeles

Citation Details

Gleason, K. E., McConnell, J. R., Arienzo, M. M., Sexstone, G. A., & Rahimi, S. (2022). Black carbon dominated dust in recent radiative forcing on Rocky Mountain snowpacks. Environmental Research Letters, 17(5), 054045.

ENVIRONMENTAL RESEARCH
LETTERS

LETTER • OPEN ACCESS

Black carbon dominated dust in recent radiative forcing on Rocky Mountain snowpacks

To cite this article: Kelly E Gleason *et al* 2022 *Environ. Res. Lett.* **17** 054045

ENVIRONMENTAL RESEARCH
LETTERS

OPEN ACCESS

RECEIVED
24 November 2021

REVISED
12 April 2022

ACCEPTED FOR PUBLICATION
19 April 2022

PUBLISHED
9 May 2022

LETTER

Black carbon dominated dust in recent radiative forcing on Rocky Mountain snowpacks

Kelly E Gleason[1,*], Joseph R McConnell[2], Monica M Arienzo[2], Graham A Sexstone[3] and Stefan Rahimi[4]

[1] Department of Environmental Science and Management, Portland State University, Portland, OR, 97207-0751, United States of America
[2] Division of Hydrologic Sciences, Desert Research Institute, 2215 Raggio Parkway, Reno, NV, 89512, United States of America
[3] U.S. Geological Survey, Colorado Water Science Center, Denver Federal Center, Lakewood, CO, 80225, United States of America
[4] Institute of Environment and Sustainability, University of California Los Angeles, Los Angeles, CA, 90095, United States of America
[*] Author to whom any correspondence should be addressed.

E-mail: k.gleason@pdx.edu

Keywords: snow hydrology, light absorbing particles, radiative forcing, snow-water resources, snowpack energy balance

Supplementary material for this article is available online

Abstract

The vast majority of surface water resources in the semi-arid western United States start as winter snowpack. Solar radiation is a primary driver of snowmelt, making snowpack water resources especially sensitive to even small increases in concentrations of light absorbing particles such as mineral dust and combustion-related black carbon (BC). Here we show, using fresh snow measurements and snowpack modeling at 51 widely distributed sites in the Rocky Mountain region, that BC dominated impurity-driven radiative forcing in 2018. BC contributed three times more radiative forcing on average than dust, and up to 17 times more at individual locations. Evaluation of 2015–2018 archived samples from most of the same sites yielded similar results. These findings, together with long-term observations of atmospheric concentrations and model studies, indicate that BC rather than dust has dominated radiative forcing by light absorbing impurities on snow for decades, indicating that mitigation strategies to reduce radiative forcing on headwater snow-water resources would need to focus on reducing winter and spring BC emissions.

1. Introduction

Snowmelt is the primary source of surface water in the semi-arid western United States [1], with high-elevation mountain snowpacks serving as crucial winter reservoirs that slowly release water to streams and rivers during the growing season in late spring and summer [2, 3]. Pristine seasonal snow is highly reflective [4–6] but even small amounts of light absorbing particles (LAP) deposited on snow darken the surface, thereby lowering albedo and increasing absorbed solar energy [7–10]. This positive radiative forcing at the snow surface drives earlier and faster snowmelt [9, 11–13] particularly as LAP concentrate on the snowpack surface in spring [14], thereby reducing water storage and advancing the timing of streamflow [15]. Enhanced snowmelt results in earlier snow disappearance, contributing to atmospheric warming because of the 'snow albedo feedback' [6, 7, 10, 16, 17] while extending periods of summer forest growth and late-summer drought. Together, these effects exacerbate late season soil moisture deficits [18] and contribute to increasing forest fire activity [19, 20].

LAP include mineral dust from desert regions and agricultural areas [14, 21], as well as black carbon (BC) from fires (wild [22–25], domestic [26]), and fossil-fuel combustion (coal, diesel) [14, 27]. Organic debris from nearby forests [28–30], together with BC and burned woody debris from standing burned forests [31–33], also contribute to LAP concentrations in snow, although effects are largely local. Mineral dust concentrations generally are much higher than BC concentrations in seasonal snow [34], but BC is orders of magnitude more effective at absorbing solar energy in the visible wavelengths (0.38–0.7 nm) [10]. Recent understanding of BC and dust concentrations in western snowpacks are based on few and spatially limited snow measurements often from areas of relatively high atmospheric dustiness [27, 34, 35]. Moreover, BC and dust rarely have been measured concurrently in western seasonal snow so

climate model simulations of the effects of LAP in snow on radiative forcing, snowmelt, and hydroclimate [36, 37] generally have been evaluated against sparse measurements of either dust or BC snow concentrations, but seldom both [11]. To reduce snow radiative forcing and preserve valuable snow-water resources in the semi-arid western United States, findings from these studies have been used to promote reductions in activities that lead to increased dust emissions including over-grazing and off-road vehicle use in sensitive areas such as the Colorado Plateau [21]. The objective of our research was to quantify the broad scale spatial variability of radiative forcing on seasonal snow by LAP and evaluate the relative contribution of BC and dust-related radiative forcing on seasonal snow across the Intermountain West.

2. Methods

To quantify the radiative forcing due to LAP in seasonal snow, we used co-registered measurements of both BC and mineral dust in snow samples collected from more than 50 widely distributed Rocky Mountain sites each year from 2015 to 2018, together with snowpack radiative transfer modeling (figure 1).

2.1. Measuring light absorbing particles in snow

As part of the ongoing U.S. Geological Survey Rocky Mountain Snowpack Chemistry project (https://co.water.usgs.gov/projects/RM_snowpack), column-integrated snow samples were collected between 2015 and 2018 at more than 50 alpine and sub-alpine sampling sites located between 36° N and 49° N latitude, and between 115° W and 105° W longitude (table S1 available online at stacks.iop.org/ERL/17/054045/mmedia), with the number of sites slightly varying from year to year. Near surface samples of the upper 30 cm and surface samples also were collected in 2018. All snow samples were collected using sterile techniques and as near as possible to peak snow water equivalent (SWE) accumulation. At each location, snowpack parameters including snow density, snow depth, and SWE were collected, and data are available in the U.S. Geological Survey National Water Information System (https://doi.org/10.5066/F7P55KJN). Snowmelt processing for 2018 and LAP analyses for all years were subsequently completed at the Desert Research Institute Ice Core Laboratory. Samples collected in 2018 were kept frozen until immediately prior to analysis in the lab. Samples from 2015 to 2017, as well as a split of the 2018 samples, were melted, refrozen, and archived until 2018 when they were melted immediately prior to analysis.

We evaluated LAP concentrations in the snow samples using three primary measurements: (a) BC mass concentrations using the well-established single-particle incandescence method originally developed for ice-core analyses [38], (b) mineral dust mass concentrations based on semi-quantitative, size-resolved insoluble particle measurements [39] and confirmed using total cerium concentration measurements [40], and (c) organic and inorganic mass concentrations of large particles using gravimetric filtering and loss-on-ignition, similar to 'dust' measurements reported in much of the literature [9, 21, 41]. Although LAP concentrations of BC and dust were used to determine radiative forcing on snow by LAP, we also calculated depositional fluxes (LAP concentration multiplied by annual snow accumulation) to facilitate understanding of potential sources [42].

To ensure uniformity in the column-integrated sample, we melted, homogenized, and then divided the samples into three sub-samples with separate vials for different analyses. To evaluate the mass of small LAP including BC and mineral dust, the first sub-sample was analyzed using a continuous flow analysis system similar to that used for ice core measurements [43]. Samples were pumped through a 20 μm stainless steel filter to remove large particles and prevent clogging the sample lines, and then into a low-volume debubbler. From the debubbler, the sample stream was split for measurements of BC approximately in the size range of 0.09–0.6 μm using an incandescence-based Single Particle Soot Photometer® (SP2; Droplet Measurement Technologies), and insoluble particles using an Abakus® laser-based particle counter (Abakus) that determines semi-quantitative, size-resolved particle counts in the size range 0.8–10 μm [44].

BC calibrations were conducted twice daily using three different standard concentrations. Under-recovery during measurements of BC concentrations in snow samples that have been melted and refrozen is well known [45], so our study primarily focused on 2018 when fresh, previously unmelted samples (BC_{fresh}) were available. To extend the analysis over three additional years, however, we also analyzed previously melted and refrozen archived samples obtained from most of the same sites each year from 2015 through 2018 (BC_{recov}), but corrected the measurements of BC for under-recovery using a correction factor of 2.72 determined by comparing measurements in the fresh and archived samples from 2018 collected from the same snowpit face (figure S1). The under-recovery or 'undercatch' we observed was in the range of previously documented BC loss in snow samples from hydrophobic particles adhering to the bottle walls [45]. This correction also accounts for observed loss of BC which may be due to the refreezing of the archived snow samples and associated structural changes in measured BC. All BC measurements in refrozen samples therefore were approximately corrected for under-recovery (BC_{recov}) by multiplying the measured concentrations by the 2.72 factor. For completeness, results from both fresh and archived 2018 samples are shown in figure S1. A similar evaluation of mineral dust recovery showed

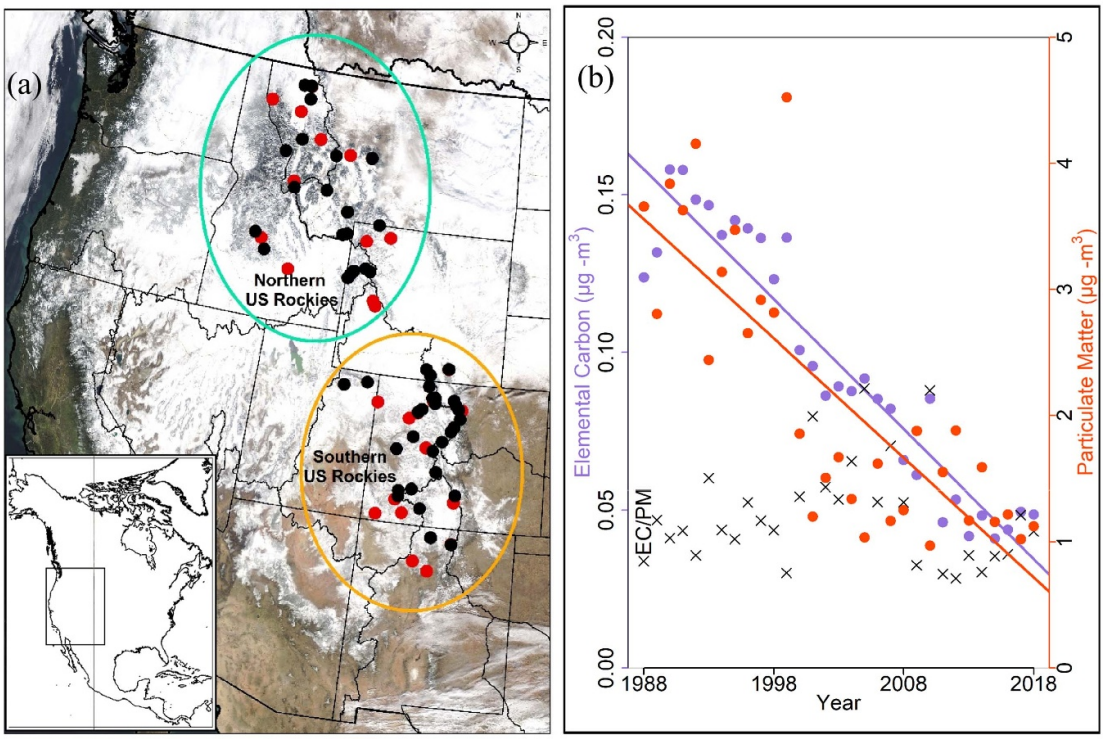

Figure 1. Snow sampling across the Rocky Mountain seasonal snow zone in the western United States. (a) Moderate Resolution Imaging Spectroradiometer (MODIS) satellite image of true color corrected reflectance showing seasonal snow cover on 27 January 2017 obtained from NASA Worldview. Shown are 2018 snow sampling (filled black circles) sites and Interagency Monitoring of Protected Visual Environments (IMPROVE) long-term atmospheric aerosol measurement sites (filled red circles) in the northern (cyan) and southern (yellow) Rocky Mountains. (b) Averaged 1988–2018 IMPROVE measurements available at, http://vista.cira.colostate.edu/Improve/, indicate declines in winter-season (January, February, and March) elemental carbon (EC) as a BC proxy (purple) and particulate matter (PM) as a dust proxy (orange). The EC/PM ratio (black) shows no trend, indicating similar, ∼50% declines in wintertime atmospheric concentrations of both aerosols during the past 30 years.

no statistically significant difference (99% confidence interval) in recovery between fresh and refrozen samples. From replicate analyses of ice cores and snow samples, typical errors in BC concentration measurements with the SP2-based methods are <5% for previously unmelted samples [22, 46, 47].

The size-resolved insoluble particle counts from the Abakus were binned into four sizes for the radiative transfer model simulations (0.8–1, 1–2.5, 2.5–5, and 5–10 μm) and converted into mass-equivalent mineral dust concentrations assuming spherical particles and a density of 2650 kg m^{-3}. We verified that insoluble particle concentrations from the Abakus were composed primarily of mineral dust using measurements of total concentrations of a broad range of elements, including rock-forming rare earth elements (REE) [48]. These measurements were made on the second sub-sample using high-resolution inductively coupled plasma mass spectrometry (HR-ICP-MS; Thermo® Element 2) and following standard procedures [48]. Melted samples were transferred into acid-cleaned plastic vials in a class-100 clean room, acidified to 1% HNO_3 using concentrated ultrapure nitric acid, and stored for three months prior to analysis to allow for acid leaching [49]. Ultrapure nitric acid spiked with indium was used as an internal standard and introduced to the sample line just prior to sample injection into the HR-ICP-MS instrument. Comparisons between insoluble particle and REE concentrations including cerium, praseodymium, gadolinium, and dysprosium, indicated that the insoluble particles measured by the Abakus were composed largely of crustal dust (e.g. comparing cerium and insoluble particle concentrations, $r = 0.67$, $p < 0.01$).

To compare these dust measurements based on insoluble particle concentrations to other published work in snow hydrology [21, 34, 35], we analyzed the third sub-sample to determine the mass and organic composition of larger impurities in the snowpack. The samples were melted in Whirl-Pak bags and vacuum-filtered using Whatman® Grade GF/F glass fiber filters (average pore space 0.7 μm). Using loss-on-ignition to distinguish organic versus inorganic debris concentrations on snowpack [50], the filters were combusted in a muffle furnace for two hours at 530 °C and the organic debris calculated as the difference in mass before and after combustion.

2.2. Modeling radiative forcing from light absorbing particles in snow

To estimate the additional solar energy absorbed by a snowpack as a result of relative contributions of BC and mineral dust, we used

the well-established Snow, Ice, and Aerosol Radiation (SNICAR) model [16, 51] available online at http://github.com/EarthSciCode/SNICARv2 and the measured LAP concentrations assuming that the impurities were distributed uniformly within the snowpack. SNICAR uses a two-stream radiative transfer solution [52] to calculate snow albedo with known concentrations of BC and dust, snow-grain size, and incident-solar-flux characteristics. Radiative forcing of snow is determined primarily by smaller particles [10, 53], so only the BC and size-resolved mineral dust concentrations were used in the SNICAR modeling, not the large particle concentrations determined by filtering and loss-on-ignition. The radiative forcing calculations were conducted assuming externally mixed uncoated BC, dust particles from 0.05 to 5.0 μm in size, and spherical snow grains. The assumption of external mixing state of LAP in snow may underestimate the overall radiative forcing contribution from BC by 30%–60% [53] and from dust by 10%–30% [54] across the visible part of the spectrum in snow. In addition, the assumption of spherical snow grains may increase the radiative forcing from BC in snow by up to 31% [53] and from dust in snow by up to 45% [54] relative to non-spherical snow grains.

To isolate the impacts of LAP variability on radiative forcing from geographic location (e.g. slope, aspect, latitude), we calculated the snow albedo for LAP-impacted and pristine snow using consistent parameters for snowpack and LAP condition in SNICAR for each site location (i.e. effective grain size of 200 μm, snowpack density of 250 kg m^{-3}). These parameters were chosen as representative of mid-winter Rocky Mountain snowpack conditions before substantial grain growth and snowpack densification occurs during ablation [41, 55]. For each sampling location the solar zenith angle was derived from the University of Oregon Solar Radiation Monitoring Laboratory Solar Position Calculator Tool available online at http://solardata.uoregon.edu/SolarPositionCalculator.html. Radiative forcing was calculated as the difference in net shortwave radiation at the snow surface between modeled albedo values of snow with and without LAP impurities and using daily radiation values on March 21 near the spring equinox for all years sampled as a representative consistent date for the snow sample collection.

An alpha value of 0.01 was used throughout this study as a measure of significance. All geospatial analysis was conducted using ArcInfo 10.4.1 [56]. All statistical analyses were conducted using R software [57].

3. Results

BC concentrations measured in the previously unmelted, column-integrated 2018 samples (BC_{fresh}) ranged from 3.7 to 27.4 ng g^{-1} (mean = 7.3 ng g^{-1}, sd = 3.9 ng g^{-1}) (figure 2). While dust concentrations measured in the previously unmelted, column-integrated 2018 samples ($dust_{fresh}$) were 10–100 times higher ranging from 0.05 to 1.9 μg g^{-1} (mean = 0.61 μg g^{-1}, sd = 0.47 μg g^{-1}) (figure 2). Concentrations generally were higher in the surface and near-surface samples, with BC_{fresh} concentrations ranging from 1.4 to 78.3 ng g^{-1} (mean = 9.8 ng g^{-1}, sd = 13.0 ng g^{-1}) and from 1.5 to 20.7 ng g^{-1} (mean = 6.6 ng g^{-1}, sd = 4.5 ng g^{-1}) in the surface and near-surface samples, respectively (table S2). Dust concentrations ranged from 0.03 to 10.3 μg g^{-1} (mean = 0.9 μg g^{-1}, sd = 0.7 μg g^{-1}) in the surface samples and from 0.05 to 3.9 μg g^{-1} (mean = 0.6 μg g^{-1}, sd = 0.7 μg g^{-1}) in the near-surface samples (table S2). These dust concentrations are comparable to those reported from 1993 to 2014 for some of the same sites [58], but with differences in measurement methodologies. Organic and inorganic debris concentrations in the 2018 column-integrated samples (figure S2) ranged from 0.5 to 300 μg g^{-1} (mean = 30 μg g^{-1}, sd = 50 μg g^{-1}) and 0.5–40 μg g^{-1} (mean = 20 μg g^{-1}, sd = 010 μg g^{-1}), respectively. Although spatially variable, these concentrations also were consistent with the few previously reported measurements at nearby sampling sites [21, 35].

The snowpack measurements and SNICAR modeling show that BC was the dominate driver of radiative forcing at nearly all of the sampling sites in 2018 (figure 2), with BC greater than dust-driven forcing at 48, 50, and 50 of the 51 sites for integrated, near-surface and surface samples, respectively (table S2). For the column-integrated samples, the average ratio of BC to dust-driven forcing was 3.0 (sd = 2.4), with ratios varying from 0.9 to 17.1. Total SNICAR-simulated radiative forcing from BC and mineral dust in the snowpack ranged from 1.8 to 10.4 W m^{-2} (mean = 3.9 W m^{-2}, sd = 1.6 W m^{-2}) (figure 2), with average hourly BC-driven radiative forcing of 1.6–9.1 W m^{-2} (mean = 3.1 W m^{-2}, sd = 1.2 W m^{-2}) and dust-driven forcing ranging from 0.1 to 3.8 W m^{-2} (mean = 1.4 W m^{-2}, sd = 0.9 W m^{-2}) (figure S3).

Similar to the 2018 fresh snow measurements, the archived column-integrated snowpack measurements and modeling show that BC was the dominate driver of radiative forcing at more than 98% of the measurement sites between 2015 and 2018, with an average of 2.9 (sd = 1.0), and up to 7.7 times more forcing from BC than from mineral dust (figure 3). Concentrations measured in archived samples—scaled by 2.72 to correct for estimated under-recovery in BC measurements of previously melted and refrozen samples (BC_{recov}, figure S4)—ranged from 1.2 to 27.7 ng g^{-1} (mean = 6.5 ng g^{-1}, sd = 2.2 ng g^{-1}), whereas dust concentrations in these samples ranged from 0.05 to 4.3 μg g^{-1} (mean = 0.5 μg g^{-1}, sd = 0.3 μg g^{-1}, figure S5).

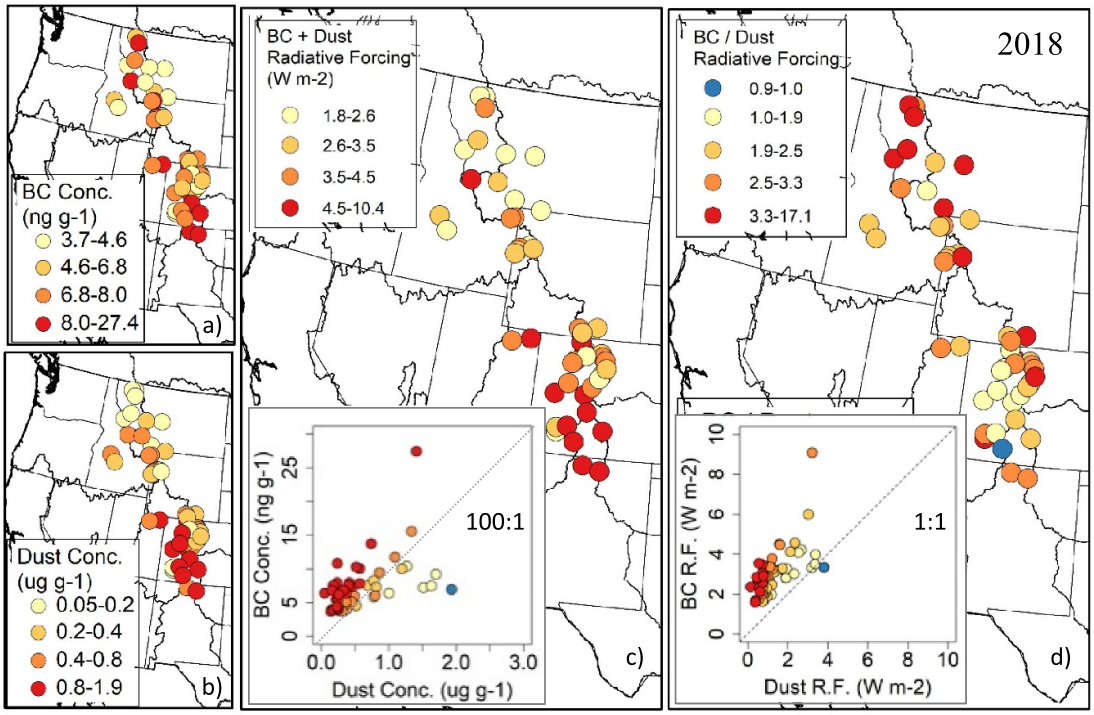

Figure 2. BC and mineral dust concentrations in 2018 fresh snow samples and associated radiative forcing on snow at 51 sampling locations (table S2). (a) BC concentration (ng g^{-1}), (b) dust concentration (μg g^{-1}), (c) sum of BC and dust-driven radiative forcing (W m^{-2}), and (d) ratio of BC to dust-driven radiative forcing (R.F.). Insets show cross plots comparing BC and dust values, with colors reflecting the ratio of BC to dust radiative forcing.

Average hourly BC-driven radiative forcing ranged from 0.1 to 9.1 W m^{-2} (mean = 2.8 W m^{-2}, sd = 0.8 W m^{-2}) (figure S6), and dust-driven forcing ranged from 0.1 to 6.5 W m^{-2} (mean = 1.2 W m^{-2}, sd = 0.5 W m^{-2}) (figure S7). Total SNICAR-simulated radiative forcing from BC and mineral dust in the snowpack ranged from 1.8 to 11.1 W m^{-2} (mean = 3.5 W m^{-2}, sd = 0.9 W m^{-2}) (figure S8), and was consistently greatest in the southern Rocky Mountains demonstrating a strong latitudinal gradient in impurity-driven radiative forcing. The BC/dust ratio was greatest in the northern Rocky Mountains but with high interannual variability observed at specific sites (figure 3). Peak SWE volume also demonstrated high interannual variability across the Rocky Mountains (figure S9).

4. Discussion

BC and dust concentrations in snow measured in this study from Rocky Mountain subalpine and alpine snowpacks were in the range of limited measurements of BC and dust concentrations in snow from ice cores, glaciers, and snowpacks around the world [26]. Generally, the midlatitudes have moderate and highly variable LAP concentrations similar to those found in this study [8, 27]. In remote locations such as Antarctica and Greenland, LAP concentrations were up to an order of magnitude lower than observed in this study [26, 38, 59]. Specific locations, such as the Tianshan Mountains central Asia for BC, or the southern Rockies in central North America for dust, have exceptionally high periodic LAP concentrations, particularly during the spring ablation period [8, 26].

Previous BC-on-snow studies demonstrated how even small BC concentrations can profoundly increase the solar radiation absorbed by the snowpack [10, 16, 38]. At only one of the 51 sites in 2018—Wolf Creek Pass, located in the San Juan Mountains of southwest Colorado—was the radiative forcing on winter snow from dust greater than that from BC concentrations (table S1). This site had the highest $dust_{fresh}$ concentration of all sites (0.9 μg g^{-1}), which is consistent with previous work [21] focused on the nearby Senator Beck Basin in the San Juan Mountains [60]. BC_{recov} dominated the radiative forcing on winter snow in 54 of 55 sites in 2015, 57 of 57 sites in 2016, 56 of 57 sites in 2017, and 55 of 57 sites in 2018, sampled across the West (figure 3, table S1). The 1.8% of archived snow sample sites where $dust_{recov}$ dominated BC_{recov} impurity-driven radiative forcing, included Four Mile Meadow located in western Wyoming, and Ripple Creek and Slumgullion Pass, located in western Colorado, both near agricultural dust sources.

LAP concentrations at isolated locations may not accurately represent larger regions, however, or the associated regional radiative forcing [21, 34, 35]. To place the point snowpack measurements in larger spatial perspective, we also compared the snowpack

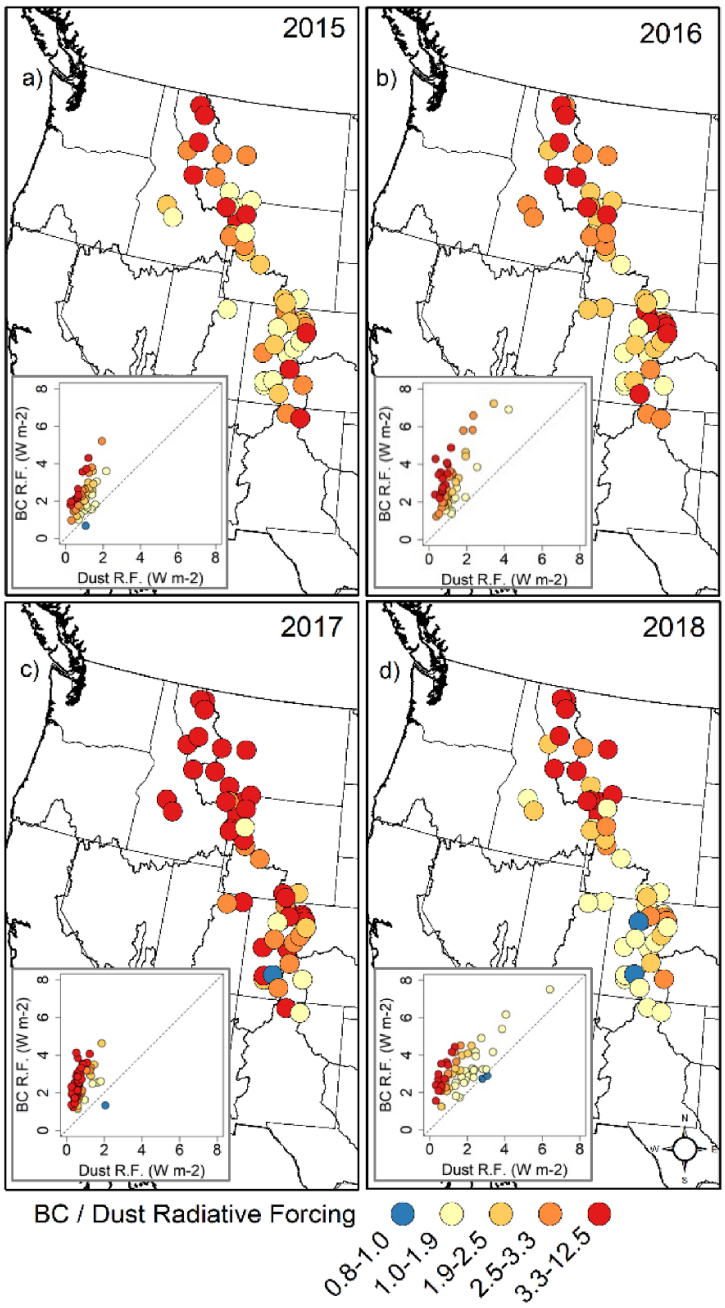

Figure 3. Ratio of BC to mineral dust-driven radiative forcing of snow from 2015 to 2018 (table S1). Radiative forcing was calculated using recovery-corrected BC and dust concentrations measured in archived snow samples from (a) 2015, (b) 2016, (c) 2017, and (d) 2018. Color scale is the same as for 2018 fresh snow samples (figure 2(d)). Insets show cross plots comparing BC and dust values.

measurements with modelled BC and dust values in snow previously reported by [37]. These were based on 2009 simulations across a large area of the Rocky Mountains using the Weather Research and Forecasting model coupled with Chemistry (WRF-Chem) on a 4 km grid. [37] found that BC dominated perturbations to the snow surface energy balance compared to dust for 2009 when integrated over mountainous terrain by more than 2 W m^{-2}. Consistent with our results, [37] found dust concentrations in snow decreased northward, unlike BC concentrations in snow, due to the southern Rockies proximity to dust emission sources. The WRF-Chem modeling concluded that BC radiative forcing dominated dust radiative forcing, leading to BC-related snow darkening which lead to earlier snowmelt, earlier snow disappearance, and earlier associated streamflow across the Rocky Mountains [37].

Our measurements clearly indicate that forcing from BC dominated overall snowpack radiative forcing throughout much of the Rocky Mountain region between 2015 and 2018, but earlier samples are not available to extend these findings. To place the 2015–2018 LAP measurements reported here in a longer temporal context, we instead evaluated the 1988–2018 winter-season (January, February,

and March) records of atmospheric BC and mineral dust aerosols from the Interagency Monitoring of Protected Visual Environments (IMPROVE) network [61] at sites from similar regions of the Rocky Mountains as the snowpack measurements. IMPROVE data were obtained from the online data portal at, http://vista.cira.colostate.edu/Improve/. For BC and dust comparisons, we used elemental carbon fraction (EC) and particulate matter (PM10-2.5) from the IMPROVE observations, respectively (figure 1). Regional patterns in the IMPROVE measurements are consistent with the general trends in the snowpack-derived BC and dust concentrations, with EC concentrations in the southern Rockies twice those in the northern Rockies (0.04 compared to 0.02 μg m^{-3}) and PM10-2.5 concentrations about 25% higher (3.2 compared to 2.7 μg m^{-3}). However, we observed no consistent site-to-site relationship when comparing 2018 atmospheric EC values with snowpack BC_{fresh} measurements at sites located within 20 km or less of each other, or when comparing atmospheric PM10-2.5 with snowpack dust measurements. For the longer 2015–2018 period represented by the archived snow samples, we found weak relationships between EC and 2015–2018 archived BC_{recov} concentrations ($R^2 = 0.1$, $p < 0.0001$), and somewhat stronger relationships between PM10-2.5 and snowpack $dust_{recov}$ concentrations ($R^2 = 0.21$, $p < 0.0001$). Further evaluation using semi-variogram analyses identified weak, broad-scale regional spatial autocorrelation of the snowpack-derived BC_{fresh} concentrations, and no spatial autocorrelation of snowpack-derived $dust_{fresh}$ concentrations (figure S10). Similar evaluation of atmospheric EC and PM10-2.5 measurements showed no spatial autocorrelation at any scale, suggesting that local atmospheric emissions overwhelm any regional variations in dust and BC concentrations (figure S11).

5. Conclusions

As the American West continues to endure a multi-decadal megadrought [62], extreme heat waves [63, 64], and unrelenting large wildfires [65, 66], snow-water resources are more important than ever for water security [67]. Our findings, developed from detailed measurements of combustion-related BC and mineral dust in snow samples collected from more than 50 widely distributed Rocky Mountain locations and consistent with WRF-Chem model simulations, demonstrate that BC-driven radiative forcing was three times greater than dust-driven forcing on average across sampling sites every year from 2015 through 2018. Evaluation of atmospheric measurements from the IMPROVE network, moreover, indicate that although wintertime concentrations of both dust and BC-related aerosols have broadly declined by ~50% between 1988 to 2018, BC-driven forcing has dominated dust-driven radiative forcing for decades (figures 1 and S11). Our analysis indicates a contrary trend in dust aerosols from Clow *et al* [58], who found site specific variability, with overall increases in dust particularly in the southern Rockies. We note that they examine a shorter time period (1993–2014) and a different parameter (fine-soil component of dust aerosols) from IMPROVE data [58]. Because snow darkening from LAP increases net shortwave radiation at the snow surface which ultimately enhances snowmelt particularly during late spring and early summer, these findings indicate that mitigation strategies to retain important snow-water resources in the Rocky Mountains would need to focus on reducing winter and spring LAP emissions—especially those processes responsible for BC emissions such as domestic wood burning and fossil-fuel combustion in the region.

Data availability statement

All data that support the findings of this study are included within the article (and any supplementary files).

Acknowledgments

Funding for this research was provided by the Sulo and Aileen Maki Endowment at the Desert Research Institute. Snow sampling was supported by the U.S. Geological Survey (USGS) in cooperation with the National Park Service, U.S. Forest Service, Colorado Department of Public Health and Environment, and Teton Conservation District. All data were analyzed by the Desert Research Institute (DRI) and are available in supplemental information or by contacting the corresponding author. Snowpack measurements collected in the field by USGS are available in the National Water Information System (https://doi.org/10.5066/F7P55KJN). We thank Colin Penn and Evan Gohring of the USGS for collecting snow measurements and the USGS for sharing the archived snow samples. Any use of trade, firm, or product names is for descriptive purposes only and does not imply endorsement by the U.S. Government.

ORCID iD

Kelly E Gleason https://orcid.org/0000-0001-5619-7568

References

[1] Serreze M, Clark M, Armstrong R, McGinnis D and Pulwarty R 1999 Characteristics of the western United States snowpack from snowpack telemetry (SNOTEL) data *Water Resour. Res.* **35** 2145–60

[2] Barnett T P, Adam J C and Lettenmaier D P 2005 Potential impacts of a warming climate on water availability in snow-dominated regions *Nature* **438** 303–9

[3] Viviroli D, Dürr H H, Messerli B, Meybeck M and Weingartner R 2007 Mountains of the world, water towers for humanity: typology, mapping, and global significance *Water Resour. Res.* **43** W07447
[4] Groisman P Y, Karl T R, Knight R W and Stenchikov G L 1994 Changes of snow cover, temperature, and radiative heat balance over the Northern Hemisphere *J. Clim.* **7** 1633–56
[5] Fernandes R, Zhao H, Wang X, Key J, Qu X and Hall A 2009 Controls on Northern Hemisphere snow albedo feedback quantified using satellite Earth observations *Geophys. Res. Lett.* **36** L21702
[6] Qu X and Hall A 2006 Assessing snow albedo feedback in simulated climate change *J. Clim.* **19** 2617–30
[7] Hansen J and Nazarenko L 2004 Soot climate forcing via snow and ice albedos *Proc. Natl Acad. Sci.* **101** 423–8
[8] Skiles S M, Flanner M, Cook J M, Dumont M and Painter T H 2018 Radiative forcing by light-absorbing particles in snow *Nat. Clim. Change* **8** 964–71
[9] Painter T H, Barrett A P, Landry C C, Neff J C, Cassidy M P, Lawrence C R, McBride K E and Farmer G L 2007 Impact of disturbed desert soils on duration of mountain snow cover *Geophys. Res. Lett.* **34** L12502
[10] Warren S G and Wiscombe W J 1980 A model for the spectral albedo of snow. II: snow containing atmospheric aerosols *J. Atmos. Sci.* **37** 2734–45
[11] Qian Y *et al* 2015 Light-absorbing particles in snow and ice: measurement and modeling of climatic and hydrological impact *Adv. Atmos. Sci.* **32** 64–91
[12] Niwano M, Kajino M, Kajikawa T, Aoki T, Kodama Y, Tanikawa T and Matoba S 2021 Quantifying relative contributions of light-absorbing particles from domestic and foreign sources on snow melt at Sapporo, Japan during the 2011–2012 winter *Geophys. Res. Lett.* **48** e2021GL093940
[13] Tuzet F, Dumont M, Lafaysse M, Picard G, Arnaud L, Voisin D, Lejeune Y, Charrois L, Nabat P and Morin S 2017 A multilayer physically based snowpack model simulating direct and indirect radiative impacts of light-absorbing impurities in snow *Cryosphere* **11** 2633–53
[14] Sterle K M, McConnell J R, Dozier J, Edwards R and Flanner M 2013 Retention and radiative forcing of black carbon in eastern Sierra Nevada snow *Cryosphere* **7** 365–74
[15] Hallema D W, Sun G, Caldwell P V, Norman S P, Cohen E C, Liu Y, Bladon K D and McNulty S G 2018 Burned forests impact water supplies *Nat. Commun.* **9** 1307
[16] Flanner M, Zender C S, Hess P G, Mahowald N M, Painter T H, Ramanathan V and Rasch P J 2009 Springtime warming and reduced snow cover from carbonaceous particles *Atmos. Chem. Phys.* **9** 2481–97
[17] Hadley O L and Kirchstetter T W 2012 Black-carbon reduction of snow albedo *Nat. Clim. Change* **2** 437–40
[18] Harpold A A 2016 Diverging sensitivity of soil water stress to changing snowmelt timing in the western US *Adv. Water Resour.* **92** 116–29
[19] Westerling A, Hidalgo H, Cayan D and Swetnam T 2006 Warming and earlier spring increase western US forest wildfire activity *Science* **313** 940–3
[20] Littell J S, Peterson D L, Riley K L, Liu Y and Luce C H 2016 A review of the relationships between drought and forest fire in the United States *Glob. Change Biol.* **22** 2353–69
[21] Painter T H, Skiles S M, Deems J S, Bryant A C and Landry C C 2012 Dust radiative forcing in snow of the Upper Colorado River Basin: 1. A 6 year record of energy balance, radiation, and dust concentrations *Water Resour. Res.* **48** W07521
[22] Arienzo M, McConnell J R, Murphy L N, Chellman N, Das S, Kipfstuhl S and Mulvaney R 2017 Holocene black carbon in Antarctica paralleled Southern Hemisphere climate *J. Geophys. Res.: Atmos.* **122** 6713–28
[23] Hegg D A, Warren S G, Grenfell T C, Doherty S J and Clarke A D 2010 Sources of light-absorbing aerosol in arctic snow and their seasonal variation *Atmos. Chem. Phys.* **10** 10923–38
[24] Keegan K M, Albert M R, McConnell J R and Baker I 2014 Climate change and forest fires synergistically drive widespread melt events of the Greenland ice sheet *Proc. Natl Acad. Sci.* **111** 7964–7
[25] Kaspari S, McKenzie Skiles S, Delaney I, Dixon D and Painter T H 2015 Accelerated glacier melt on Snow Dome, Mount Olympus, Washington, USA, due to deposition of black carbon and mineral dust from wildfire *J. Geophys. Res.: Atmos.* **120** 2793–807
[26] Kang S, Zhang Y, Qian Y and Wang H 2020 A review of black carbon in snow and ice and its impact on the cryosphere *Earth Sci. Rev.* **210** 103346
[27] Chellman N, McConnell J R, Arienzo M, Pederson G T, Aarons S M and Csank A 2017 Reassessment of the upper fremont glacier ice-core chronologies by synchronizing of ice-core-water isotopes to a nearby tree-ring chronology *Environ. Sci. Technol.* **51** 4230–8
[28] Hardy J, Melloh R, Robinson P and Jordan R 2000 Incorporating effects of forest litter in a snow process model *Hydrol. Process.* **14** 3227–37
[29] Winkler R, Boon S, Zimonick B and Baleshta K 2010 Assessing the effects of post-pine beetle forest litter on snow albedo *Hydrol. Process.* **24** 803–12
[30] Melloh R A, Hardy J P, Davis R E and Robinson P B 2001 Spectral albedo/reflectance of littered forest snow during the melt season *Hydrol. Process.* **15** 3409–22
[31] Gleason K and Nolin A 2016 Charred forests accelerate snow albedo decay: parameterizing the post-fire radiative forcing on snow for three years following fire *Hydrol. Process.* **30** 3855–70
[32] Gleason K, Nolin A and Roth T 2013 Charred forests increase snowmelt: effects of burned woody debris and incoming solar radiation on snow ablation *Geophys. Res. Lett.* **40** 4654–61
[33] Gleason K E, McConnell J R, Arienzo M M, Chellman N and Calvin W M 2019 Four-fold increase in solar forcing on snow in western US burned forests since 1999 *Nat. Commun.* **10** 2026
[34] Skiles S M and Painter T H 2018 Assessment of radiative forcing by light-absorbing particles in snow from *in situ* observations with radiative transfer modeling *J. Hydrometeorol.* **19** 1397–409
[35] Skiles S M, Painter T H, Belnap J, Holland L, Reynolds R L, Goldstein H L and Lin J 2015 Regional variability in dust-on-snow processes and impacts in the Upper Colorado River Basin *Hydrol. Process.* **29** 5397–413
[36] Wu C, Liu X, Lin Z, Rahimi-Esfarjani S R and Lu Z 2018 Impacts of absorbing aerosol deposition on snowpack and hydrologic cycle in the Rocky Mountain region based on variable-resolution CESM (VR-CESM) simulations *Atmos. Chem. Phys.* **18** 511–33
[37] Rahimi S, Liu X, Zhao C, Lu Z and Lebo Z J 2020 Examining the atmospheric radiative and snow-darkening effects of black carbon and dust across the Rocky Mountains of the United States using WRF-Chem *Atmos. Chem. Phys.* **20** 10911–35
[38] McConnell J, Edwards R, Kok G L, Flanner M G, Zender C S, Saltzman E S, Banta J R, Pasteris D R, Carter M M and Kahl J D W 2007 20th-Century industrial black carbon emissions altered arctic climate forcing *Science* **317** 1381–4
[39] Ruth U, Wagenbach D, Steffensen J P and Bigler M 2003 Continuous record of microparticle concentration and size distribution in the central Greenland NGRIP ice core during the last glacial period *J. Geophys. Res.: Atmos.* **108** D3, 4098
[40] McConnell J R and Edwards R 2008 Coal burning leaves toxic heavy metal legacy in the Arctic *Proc. Natl Acad. Sci.* **105** 12140–4
[41] Skiles S and Painter T 2017 Daily evolution in dust and black carbon content, snow grain size, and snow albedo during snowmelt, Rocky Mountains, Colorado *J. Glaciol.* **63** 118–32
[42] Wolff E, Hall J S, Mulvaney R, Pasteur E C, Wagenbach D and Legrand M 1998 Relationship between chemistry of air,

fresh snow and firn cores for aerosol species in coastal Antarctica *J. Geophys. Res.: Atmos.* **103** 11057–70
[43] McConnell J R *et al* 2017 Synchronous volcanic eruptions and abrupt climate change ∼17.7 ka plausibly linked by stratospheric ozone depletion *Proc. Natl Acad. Sci.* **114** 10035–40
[44] Neff J, Ballantyne A P, Farmer G L, Mahowald N M, Conroy J L, Landry C C, Overpeck J T, Painter T H, Lawrence C R and Reynolds R L 2008 Increasing eolian dust deposition in the western United States linked to human activity *Nat. Geosci.* **1** 189–95
[45] Doherty S, Warren S, Grenfell T, Clarke A and Brandt R 2010 Light-absorbing impurities in Arctic snow *Atmos. Chem. Phys.* **10** 11647–80
[46] Macdonald K *et al* 2017 Observations of atmospheric chemical deposition to high Arctic snow *Atmos. Chem. Phys.* **17** 5775–88
[47] Bisiaux M, Edwards R, McConnell J R, Curran M A J, Van Ommen T D, Smith A M, Neumann T A, Pasteris D R, Penner J E and Taylor K 2012 Changes in black carbon deposition to Antarctica from two high-resolution ice core records, 1850–2000 AD *Atmos. Chem. Phys.* **12** 4107–15
[48] Uglietti C, Gabrielli P, Olesik J W, Lutton A and Thompson L G 2014 Large variability of trace element mass fractions determined by ICP-SFMS in ice core samples from worldwide high altitude glaciers *Appl. Geochem.* **47** 109–21
[49] Arienzo M M, McConnell J R, Chellman N and Kipfstuhl S 2019 Method for correcting continuous ice-core elemental measurements for under-recovery *Environ. Sci. Technol.* **53** 5887–94
[50] Dean W E Jr 1974 Determination of carbonate and organic matter in calcareous sediments and sedimentary rocks by loss on ignition: comparison with other methods *J. Sediment. Res.* **44** 242–8
[51] Flanner M, Zender C, Randerson J and Rasch P 2007 Present-day climate forcing and response from black carbon in snow *J. Geophys. Res.: Atmos.* **112** D11202
[52] Toon O B, McKay C, Ackerman T and Santhanam K 1989 Rapid calculation of radiative heating rates and photodissociation rates in inhomogeneous multiple scattering atmospheres *J. Geophys. Res.: Atmos.* **94** 16287–301
[53] He C, Liou K and Takano Y 2018 Resolving size distribution of black carbon internally mixed with snow: impact on snow optical properties and albedo *Geophys. Res. Lett.* **45** 2697–705
[54] He C, Liou K-N, Takano Y, Chen F and Barlage M 2019 Enhanced snow absorption and albedo reduction by dust-snow internal mixing: modeling and parameterization *J. Adv. Model. Earth Syst.* **11** 3755–76
[55] Seidel F C, Rittger K, Skiles S M, Molotch N P and Painter T H 2016 Case study of spatial and temporal variability of snow cover, grain size, albedo and radiative forcing in the Sierra Nevada and Rocky Mountain snowpack derived from imaging spectroscopy *Cryosphere* **10** 1229–44
[56] ESRI 2015 ArcGIS desktop: release 10.4
[57] R Core Team 2016 R: a language and environment for statistical computing
[58] Clow D W, Williams M W and Schuster P F 2016 Increasing aeolian dust deposition to snowpacks in the Rocky Mountains inferred from snowpack, wet deposition, and aerosol chemistry *Atmos. Environ.* **146** 183–94
[59] McConnell J, Aristarain A, Banta J, Edwards P and Simoes J 2007 20th-Century doubling in dust archived in an Antarctic Peninsula ice core parallels climate change and desertification in South America *Proc. Natl Acad. Sci. USA* **104** 5743–8
[60] Painter T H, Skiles S M, Deems J S, Brandt W T and Dozier J 2018 Variation in rising limb of Colorado River snowmelt runoff hydrograph controlled by dust radiative forcing in snow *Geophys. Res. Lett.* **45** 797–808
[61] Chow J C, Watson J G, Crow D, Lowenthal D H and Merrifield T 2001 Comparison of IMPROVE and NIOSH carbon measurements *Aerosol Sci. Technol.* **34** 23–34
[62] Williams A P, Cook E R, Smerdon J E, Cook B I, Abatzoglou J T, Bolles K, Baek S H, Badger A M and Livneh B 2020 Large contribution from anthropogenic warming to an emerging North American megadrought *Science* **368** 314–8
[63] Lopez H, West R, Dong S, Goni G, Kirtman B, Lee S-K and Atlas R 2018 Early emergence of anthropogenically forced heat waves in the western United States and Great Lakes *Nat. Clim. Change* **8** 414–20
[64] Dosio A, Mentaschi L, Fischer E M and Wyser K 2018 Extreme heat waves under 1.5 °C and 2 °C global warming *Environ. Res. Lett.* **13** 054006
[65] Dennison P, Brewer S, Arnold J and Moritz M 2014 Large wildfire trends in the western United States, 1984–2011 *Geophys. Res. Lett.* **41** 2928–33
[66] Zou Y, Rasch P J, Wang H, Xie Z and Zhang R 2021 Increasing large wildfires over the western United States linked to diminishing sea ice in the Arctic *Nat. Commun.* **12** 1–12
[67] Stewart I T, Rogers J and Graham A 2020 Water security under severe drought and climate change: disparate impacts of the recent severe drought on environmental flows and water supplies in Central California *J. Hydrol.* X **7** 100054